Electronic Supplementary Information

Experimental

Materials and chemicals

Copper(II) chloride($CuCl_2$, 99.9%), sodium tetrachloropalladate(Na_2PdCl_4, 98%), sodium borohydride ($NaBH_4$, 98%), ammonium chloride (NH_4Cl), ammonium chloride-^{15}N ($^{15}NH_4Cl$), phosphoric acid, *p*-aminobenzenesulfonamide, sulfamic acid, Nessler's reagent, N-(1-Naphthyl) ethylenediamine dihydrochloride, potassium sodium tartrate, potassium nitrate (KNO_3), potassium nitrate-^{15}N ($K^{15}NO_3$) and potassium sulfate (K_2SO_4) were obtained from Aladdin Industrial Corporation (Shanghai, China). Hydrochloric acid (36%) and ethanol (C_2H_5OH) were purchased from Beijing Chemical Works. Nafion (5 wt%) solution was purchased from Sigma-Aldrich.

Synthesis of CuPd(3:1) aerogels

Firstly, the metal precursor solution was obtained by mixing 3.75 mL of $CuCl_2$ solution (10 mM) and 1.25 mL of Na_2PdCl_4 solution (10 mM). Then, the metal precursor solution was quickly injected into 20 mL of freshly-prepared $NaBH_4$ solution (0.1 M) under stirring. After keeping stirring for 5min, the resulting black precipitates were collected by centrifugation, and washed with water and ethanol for three times, followed by dried at 50 °C in an oven overnight. The pure Cu aerogels, pure Pd aerogels, CuPd(1:1) aerogels, and CuPd(7:1) aerogels were synthesized by similar procedure except that the proportions of $CuCl_2$ solution and Na_2PdCl_4 solution were adjusted, such as 5 mL of 10 mM aqueous $CuCl_2$ for Cu aerogels, 5 mL of 10 mM aqueous Na_2PdCl_4 for Pd aerogels, 2.5 mL of 10 mM aqueous $CuCl_2$ and 2.5 mL of 10 mM aqueous Na_2PdCl_4 for CuPd(1:1) aerogels, 4.375 mL of 10 mM aqueous $CuCl_2$ and 0.625 mL of 10 mM aqueous Na_2PdCl_4 for CuPd(7:1) aerogels.

Characterizations

Scanning electron microscope (SEM) images were obtained on a ZEISS Gemini 500 SEM. A TalosS-FEG transmission electron microscope (TEM) was applied to perform characterization including TEM, high-resolution TEM (HRTEM), selected area electron diffraction (SAED), high-angle annular dark field-scanning TEM (HAADF-STEM), and energy dispersive X-ray spectroscopy (EDX) mapping analysis. X-ray diffraction (XRD) measurements were received by PANalytical X'Pert PRO equipped with a Cu Kα radiation. X-ray photoelectron spectroscopy (XPS) date were executed

utilizing a microprobe Spectrometer (ULVAC PHI Quantera) with Al Kα radiation. A TU-1900 spectrophotometer was used to record UV-Vis absorption spectra. ^{1}H NMR spectra were conducted on a superconducting-magnet NMR spectrometer (Bruker AVANCE III HD 500 MHz).

Electrochemical measurements

Electrocatalytic nitrate reduction experiments were performed on a CHI 660E electrochemical workstation using a three-electrode system (working electrode: as-made aerogels loaded on carbon paper substrate; counter electrode: Pt foil; reference electrode: saturated calomel electrode (SCE)) and a H-type electrolytic cell divided by a Nafion 211 membrane at room temperature. The catalyst ink was prepared by dispersing 5 mg of as-made aerogels in the mixture of water (490 µL), ethanol (490 µL) and 5 wt% Nafion solution (20 µL) under sonicating to obtain black suspension. To prepare the working electrode, 200 µL of catalyst ink was dropped on a piece of carbon paper (1×1 cm^2) and dried at 50 °C. When performing nitrate reduction experiments, 35 mL of 0.5 M K_2SO_4 solution with KNO_3 (50 mg L^{-1} NO$_3^-$-N) was used the cathode electrolyte, while 35 mL of 0.5 M K_2SO was used as the anode electrolyte. Polarization curves were recorded by linear scanning voltammetry (LSV) at a scan rate of 10 mV s^{-1}. The current density was obtained by normalizing the current to the geometric surface area of working electrode. Before performing potentiostatic testing, LSV is repeated with a scan rate of 10 mV s^{-1} until the curves basically coincide. The potentiostatic measurements were conducted at the different applied potentials for 2 hours, with the electrolyte in the cathodic compartment being stirred at a rate of 500 rpm during electrolysis.

Determination of products

Using a UV-Vis spectrophotometer, the ion concentration of the electrolyte solution after the potentiostat test was diluted to the appropriate concentration and measured to match the calibration curve range.[1-2]

Measurement of NO$_3^-$-N: First, 1.5 mL of the electrolyte after the constant potential test was diluted to 5 mL with water, then 0.1 mL of HCl solution (1 M) and 0.01 mL of 0.8 wt% sulfamic acid solution were added, and the color was developed for 10 min. Subsequently, the absorbance was measured by UV-Vis spectrophotometry in the wavelength range of 200 nm and 300 nm. Nitrate-N final absorbance was obtained from the following equation: A = A$_{220nm}$ -2A$_{275nm}$. Measurement of the corresponding absorbance for standard concentrations of KNO_3 solution can be used to obtain a

calibration curve.

Determination of NO$_2^-$-N: To prepare color reagents, dilute 0.4 g of p-aminobenzenesulfonamide and 0.02 g of N-(1-naphthyl)ethylenediamine dihydrochloride in a solution containing 5 mL of deionized water and 1 mL of phosphoric acid (ρ = 1.70 g/mL). Remove 0.05 mL of electrolyte and dilute to 5 mL to the range of measurement. Next, add 0.1 mL of color development reagent to the above 5 mL solution. The reagent was shaken and allowed to stand for 20 minutes before testing the absorbance by UV-Vis spectrophotometry at 540 nm. Calibration curves for different concentrations of NaNO$_2$ solution and the corresponding absorbance can be obtained.

Determination of NH$_3$-N: Nessler's reagent and a solution of potassium sodium tartrate (ρ = 500 g/L) were used as color developer for ammonium-N. First, dissolve 1 g of potassium sodium tartrate (KNaC$_4$H$_6$O$_6$-4H$_2$O) in 2 mL of ultrapure water and then dissolve by sonication. Next, remove 0.2 mL of electrolyte and dissolve up to 5 mL to reach the test range. To the above 5 mL solution, add 0.1 mL of potassium sodium tartrate solution and 0.1 mL of Nessler's reagent, shake well and let the solution develop for 20 minutes, then test the absorbance by UV-Vis spectrophotometry at 420 nm. Calibration curves were acquired by measuring the absorbance of a series of standard concentrations of NH$_4$Cl solutions.

Isotope Labeling Experiments: Isotopically labeled nitrate reduction experiments, with electrochemical nitrate reduction as described above, but with K^{15}NO$_3$ (99%) of the N source substituted. After the nitric acid reduction test, adjust the pH value of the electrolyte with 4 M sulfuric acid solution to weak acidity. To further calculate the ammonia-N concentration quantitatively, using Malay (C$_4$H$_4$O$_4$) as an external standard, ^{1}H NMR method was used to obtain the standard curve of integrated area (^{15}NH$_4^+$ -^{15}N / C$_4$H$_4$O$_4$) toward ^{15}NH$_4^+$ -^{15}N concentration. To begin with, we dissolved different amounts of ^{15}NH$_4^+$-^{15}N (10, 20, 30, 40, 50 mg L^{-1}) into 0.5 M K$_2$SO$_4$ using 120 mg L^{-1} C$_4$H$_4$O$_4$ as standard solution. Next, a mixture of 50 μL of deuterium oxide (D$_2$O) with 0.5 mL of acidified electrolyte was used to receive advance ^{1}H NMR spectra by NMR detection.

Calculate the conversion ratio of NO$_3^-$ using the following equation:

$$Conversion = \Delta c_{NO_3^-} / c_0 \times 100\% \tag{1}$$

Product selectivity is calculated by the following formula：

$$Selectivity(NH3) = c_{NH_3} / \Delta c_{NO_3^-} \times 100\% \tag{2}$$

$$Selectivity(NO2-) = c_{NO_2^-}/\Delta c_{NO_3^-} \times 100\% \qquad (3)$$

Yields of NH_3(aq) is measured using the following method：

$$Yield_{NH3} = (c_{NH_3} \times V)/(t \times m) \qquad (4)$$

Ammonia Faradaic efficiency was measured by the following formula：

$$Faradaic\ efficiency = (8F \times c_{NH_3} \times V)/(M_{NH_3} \times Q) \qquad (5)$$

The following values were used in the equations (1-5) : Δc_{NO3^-} : the concentration differential of NO_3^--N before and after the nitric acid reduction reaction; c_0 : the initial concentration of NO_3^--N in the electrolyte; c_{NO2^-}: the concentration of NO_2^- measured after the reaction; c_{NH3}: the concentration of NH_3 measured after the reaction; V: the volume of electrolyte in the cathode chamber (35 mL); t: the constant potential test time (2 hours); M_{NH3}: the molar mass of NH_3; m: the mass of loaded catalyst (1 mg), F: the Faraday constant (96,485 C mol^{-1}); Q: the charge of total electrolysis.
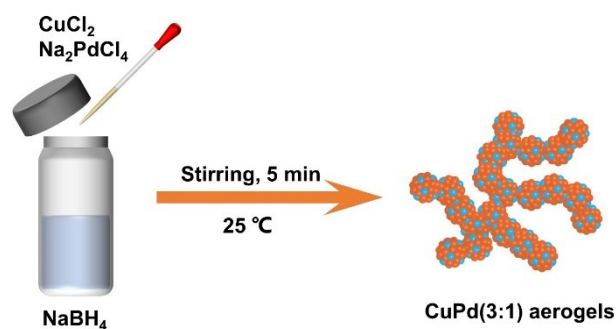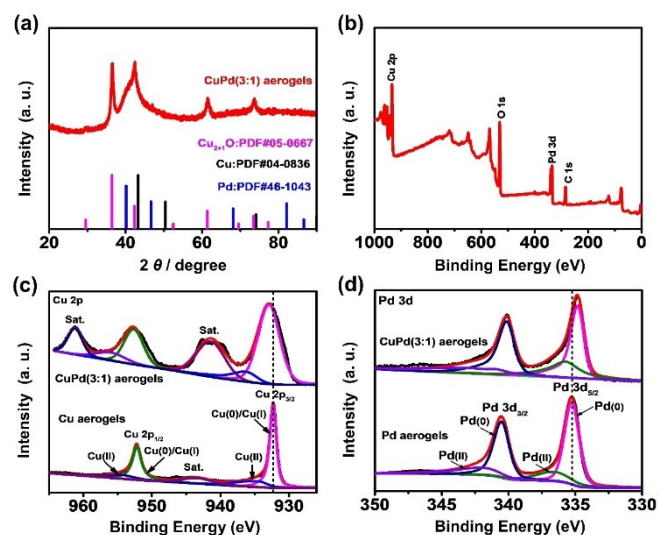
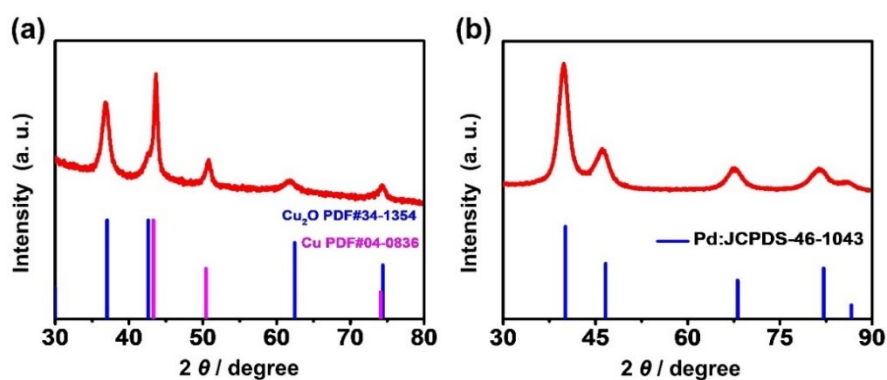**Fig. S1** Schematic illustration of the synthesis process of the CuPd(3:1) aerogels.
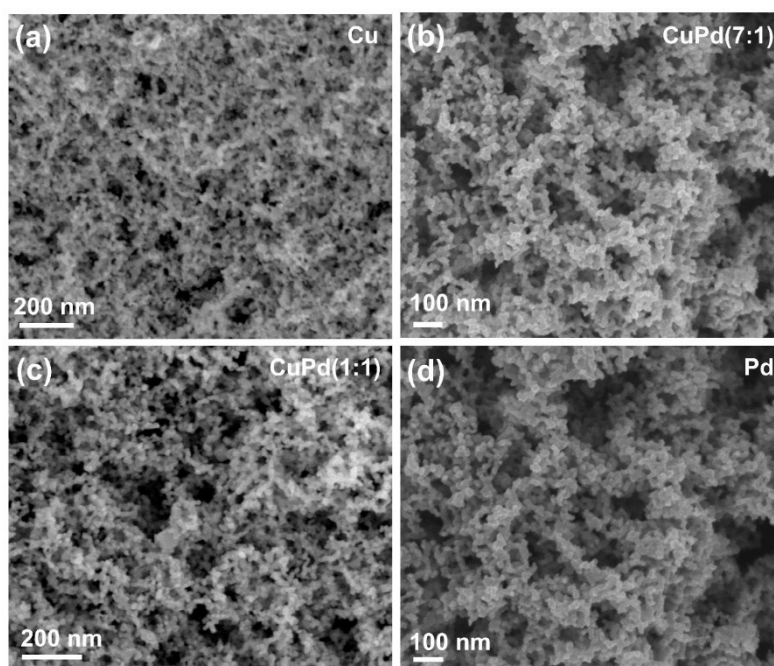
Fig. S2 SEM images of (a) pure Cu, (b) CuPd(7:1), (c) CuPd(1:1) and (d) pure Pd aerogels.
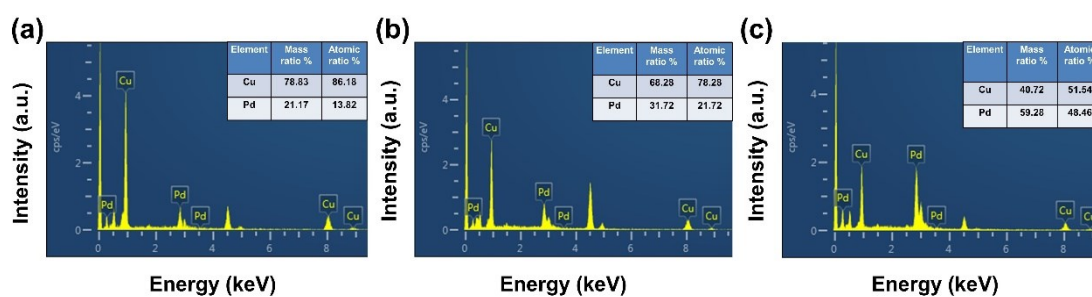
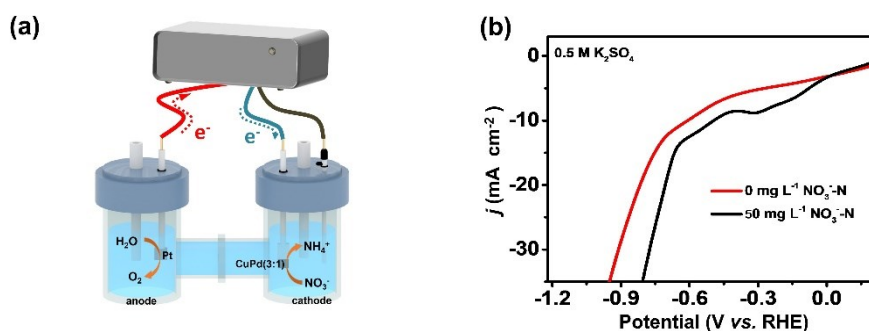**Fig. S3** EDX spectra of various aerogels: (a) CuPd(7:1), (b) CuPd(3:1), (c) CuPd(1:1).

Fig. S4 (a) XRD pattern, (b) XPS survey spectrum and the high-resolution spectra of (c) Cu 2p, (d) Pd 3d of CuPd(3:1) aerogels.
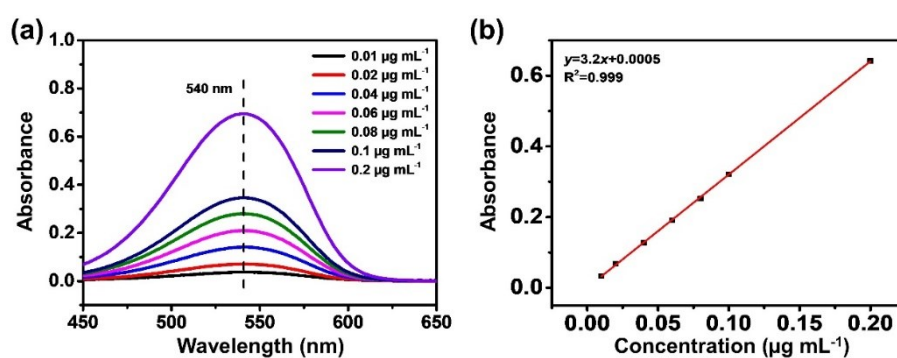

Fig. S5 XRD patterns of the (a) pure Cu and (b) pure Pd aerogels.


Fig. S6 (a) Schematic illustration of the electrocatalytic nitrate reduction system. (b) LSV curves of the CuPd(3:1) aerogels in a 0.5 M K_2SO_4 solution with or without NO_3^--N.
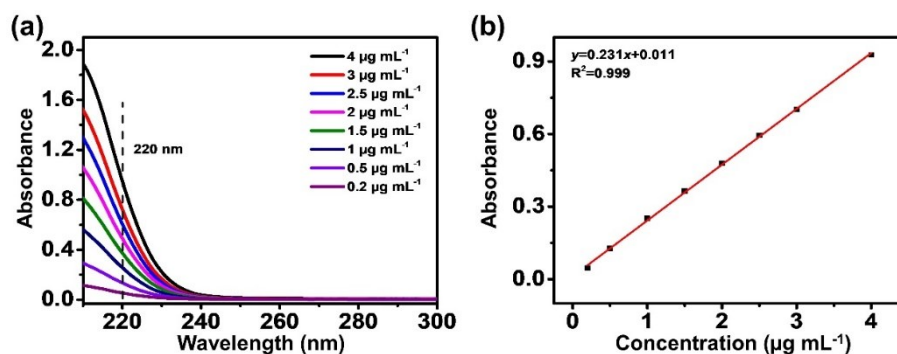
Fig. S7 (a) UV−vis absorption spectroscopy for various concentrations of NO_3^--N. (b) Calibration curve used to estimate the concentrations of NO_3^--N.


Fig. S8 (a) UV−vis absorption spectroscopy for various concentrations of NO_2^--N. (b) Calibration curve used to estimate the concentrations of NO_2^--N.
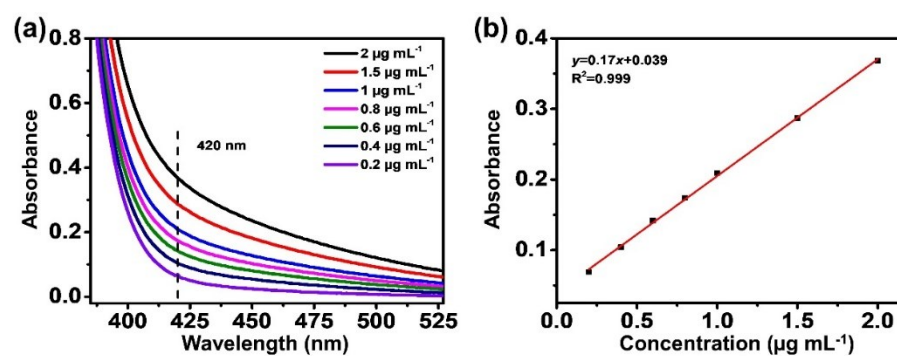
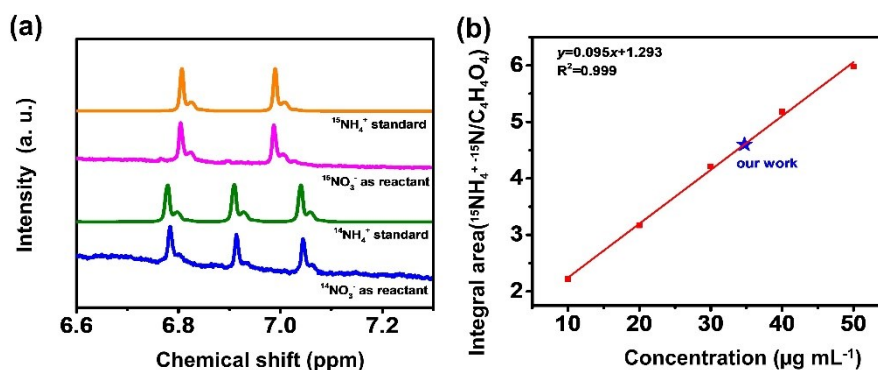**Fig. S9** (a) UV−vis absorption spectroscopy for various concentrations of NH_3-N. (b) Calibration curve used to estimate the concentrations of NH_3-N.
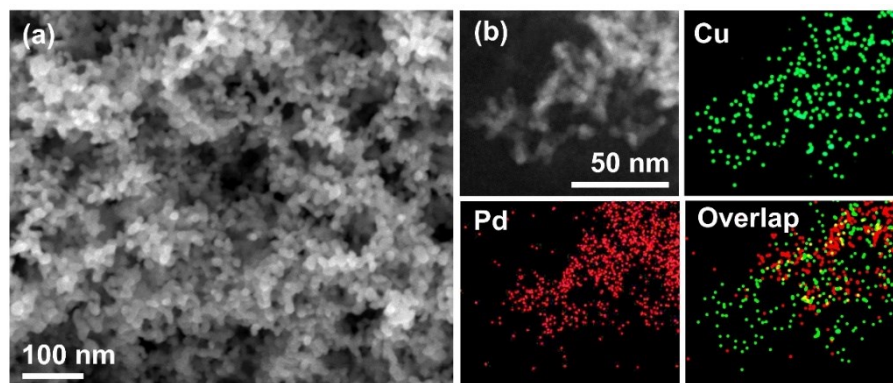
Fig. S10 (a) SEM and (b) HAADF-STEM and EDX elemental mapping images of the CuPd(3:1) aerogels after nitrate reduction stability testing.
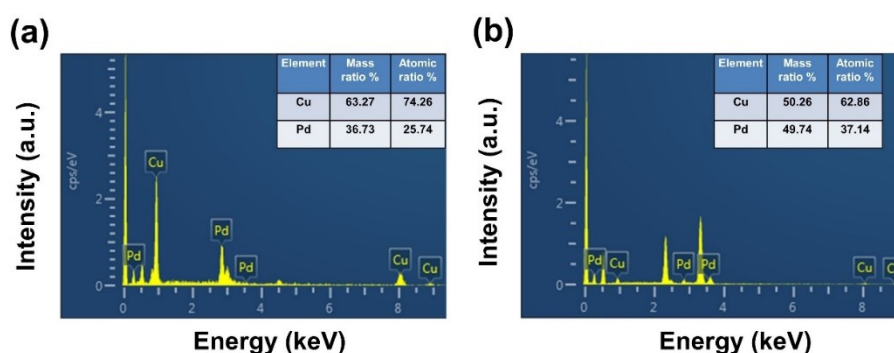
**Fig. S11** EDX spectra of CuPd(3:1) aerogels before and after the stability test.

Fig. S12 (a) ^{1}H NMR spectra of $^{15}NH_4^+$ calibration solution, $^{14}NH_4^+$ calibration solution and the electrolyte after electrocatalytic nitrate reduction using $^{15}NO_3^-$ and $^{14}NO_3^-$ as the nitrogen source. (b) The standard curve of integral area ($^{15}NH_4^+$-$^{15}N/C_4H_4O_4$) against $^{15}NH_4^+$-^{15}N concentration.

Results of the ^{1}H NMR spectrum of the post-electrolysis electrolyte with K$^{15}NO_3$ as the reactant show a characteristic double peak of $^{15}NH_4^+$, and the ^{1}H NMR spectrum of the post-electrolysis electrolyte with K$^{14}NO_3$ as the reactant exhibits a typical triple peak of $^{14}NH_4^+$ (Fig. S12a). These

results suggest that the generated ammonium is from nitrate. The concentration of ammonium produced in the electrolyte could be identified from the standard curve of the integrated area (NH_4^+-N/$C_4H_4O_4$) (Fig. S13). The concentrations of $^{15}NH_4^+$-^{15}N and $^{14}NH_4^+$-^{14}N generated by ^1H NMR quantification were almost identical compared to the colorimetric method, which confirms the accuracy of the different ammonium quantification methods (Fig. S12b).
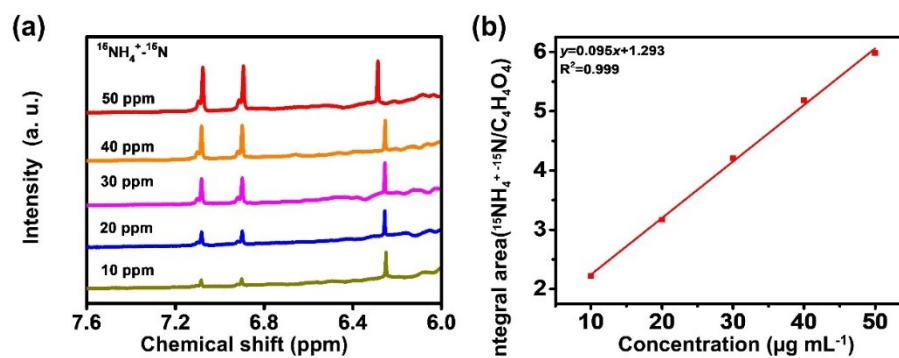
Fig. S13 (a) The ^1H NMR spectra of $^{15}NH_4^+$ with different $^{15}NH_4^+$-^{15}N concentration. (b) The standard curve of integral area ($^{15}NH_4^+$-^{15}N / $C_4H_4O_4$) against $^{15}NH_4^+$-^{15}N concentration.
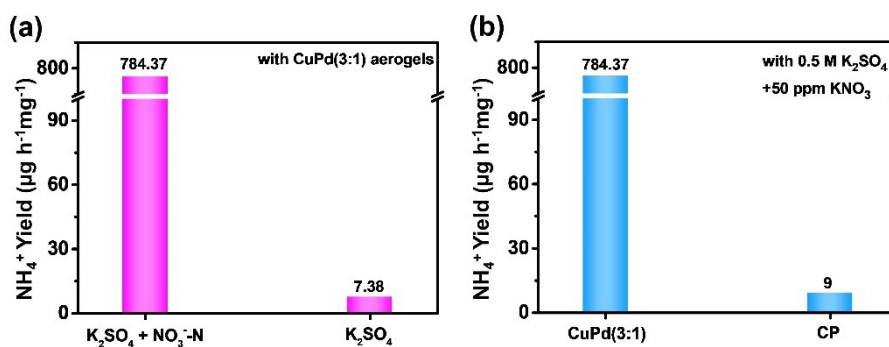
Fig. S14 (a) NH_3 yield rates of the CuPd(3:1) aerogels in 0.5 M K_2SO_4 with and without 50 mg L^{-1} NO_3^--N. (b) NH_3 yield rates of the CuPd(3:1) aerogels and blank CP.
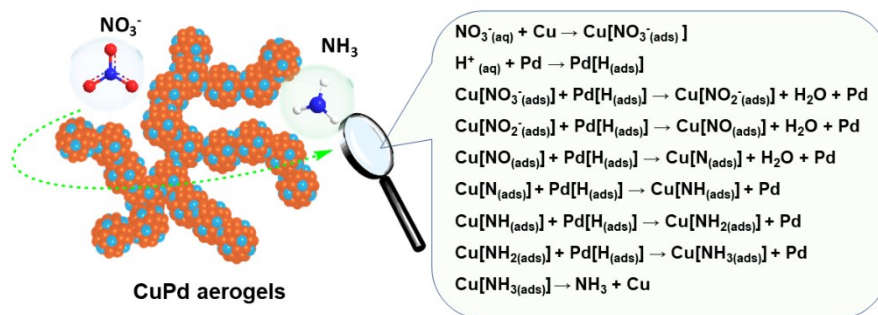
Fig. S15 Schematic illustration showing the nitrate electroreduction process over the CuPd(3:1) aerogels.

Table S1. The comparison of electrochemical nitrate reduction activity between the as-made CuPd(3:1) aerogels and some other reported electrocatalysts.

Electrocatalysts	Electrolytes	Activity	Ref.
CuPd(3:1) aerogels	**0.5 M K$_2$SO$_4$, 50 mg L^{-1} NO$_3^-$-N**	**r$_{NH3}$[a]: 784.37 μg h^{-1} mg$_{cat.}$ FE$_{NH3}$[b]: 90.02% S_{NH3}[c]: 77.49% (-0.46 V vs. RHE, 2 h)**	**This work**
O-Cu–PTCDA	0.1 M PBS, 500 ppm KNO$_3$	r$_{NH3}$: 436±85 μg h^{-1} cm^{-2} FE$_{NH3}$: 85.9% (−0.4 V vs. RHE, 4 h)	3
Cu$_{50}$Ni$_{50}$ alloy	0.1 M KOH, 10 mM KNO$_3$	FE$_{NH3}$: 93 ± 2% (0 V vs. RHE, 3 h)	4
Co$_3$O$_4$/Ti mesh	0.1 M K$_2$SO$_4$, 100 g L^{-1} KNO$_3$	r_{NH3}: 0.854 mmol h^{-1} cm^{-2} S_{NH3}: 33.6% (−0.65 V vs. RHE, 3 h)	5
Ti Electrode	0.4 M NO$_3^-$	FE$_{NH3}$: 82% (−1 V vs. RHE, 8 h)	6
Co$_3$O$_4$@NiO HNTs	0.02 M NaCl, 0.02 M NaNO$_3$	FE$_{NH3}$: 54.97% S_{NH3}: 62.29% (-1.4 V vs. SCE, 3 h)	7
Cu/Ni/20-min	0.1 M Na$_2$SO$_4$ 50 ppm NO$_3^-$-N	S_{NH3}: 66.6% (−0.6 V vs. Hg/HgO, 4 h)	8
Ni-Fe^0@Fe$_3$O$_4$	10 mM NaCl, 50 ppm NO$_3^-$	S_{NH3}: 10.4% (5 mA cm^{-2}, 4 h)	9
Iridium nanotubes	0.1 M HClO$_4$, 1 M NaNO$_3$	r$_{NH3}$: 921 μg h^{-1} mg$_{cat}^{-1}$ FE$_{NH3}$: 84.7% (0.06 V vs. RHE, 5 h)	10
Fe(20%)@NeC	50 mM Na$_2$SO$_4$ 50 mg L^{-1} NO$_3^-$-N	S_{NH3}: ＜75% (-1.3 V vs. SCE, 24 h)	11
Co$_3$O$_4$-TiO$_2$/Ti	0.1 M Na$_2$SO$_4$ 50 mg L^{-1} NO$_3^-$	S_{NH3}: ＜70% (10 mA cm^{-2}, 2h)	12

[a]ammonia yield rate; [b]ammonia Faradaic efficiency; [c]ammonia-N selectivity.

References

(1) Jia, R.; Wang, Y.; Wang, C.; Ling, Y.; Yu, Y.; Zhang, B. Boosting Selective Nitrate Electroreduction to Ammonium by Constructing Oxygen Vacancies in TiO_2. *ACS Catal.* **2020,** *10* (6), 3533-3540.

(2) Wang, Y.; Zhou, W.; Jia, R.; Yu, Y.; Zhang, B. Unveiling the Activity Origin of a Copper-based Electrocatalyst for Selective Nitrate Reduction to Ammonia. *Angew. Chem. Int. Ed. Engl.* **2020,** *59* (13), 5350-5354.

(3) Chen, G.-F.; Yuan, Y.; Jiang, H.; Ren, S.-Y.; Ding, L.-X.; Ma, L.; Wu, T.; Lu, J.; Wang, H. Electrochemical reduction of nitrate to ammonia via direct eight-electron transfer using a copper–molecular solid catalyst. *Nat. Energy* **2020,** *5* (8), 605-613.

(4) Wang, Y.; Xu, A.; Wang, Z.; Huang, L.; Li, J.; Li, F.; Wicks, J.; Luo, M.; Nam, D. H.; Tan, C. S.; Ding, Y.; Wu, J.; Lum, Y.; Dinh, C. T.; Sinton, D.; Zheng, G.; Sargent, E. H. Enhanced Nitrate-to-Ammonia Activity on Copper-Nickel Alloys via Tuning of Intermediate Adsorption. *J. Am. Chem. Soc.* **2020,** *142* (12), 5702-5708.

(5) Wang, Y.; Yu, Y.; Jia, R.; Zhang, C.; Zhang, B. Electrochemical synthesis of nitric acid from air and ammonia through waste utilization. *Natl. Sci. Rev.* **2019,** *6* (4), 730-738.

(6) McEnaney, J. M.; Blair, S. J.; Nielander, A. C.; Schwalbe, J. A.; Koshy, D. M.; Cargnello, M.; Jaramillo, T. F. Electrolyte Engineering for Efficient Electrochemical Nitrate Reduction to Ammonia on a Titanium Electrode. *ACS Sustainable Chem. Eng.* **2020,** *8* (7), 2672-2681.

(7) Wang, Y.; Liu, C.; Zhang, B.; Yu, Y. Self-template synthesis of hierarchically structured Co_3O_4@NiO bifunctional electrodes for selective nitrate reduction and tetrahydroisoquinolines semi-dehydrogenation. *Sci. China Mater.* **2020,** *63* (12), 2530-2538.

(8) Shih, Y.-J.; Wu, Z.-L.; Huang, Y.-H.; Huang, C.-P. Electrochemical nitrate reduction as affected by the crystal morphology and facet of copper nanoparticles supported on nickel foam electrodes (Cu/Ni). *Chem. Eng. J.* **2020,** *383*, 123157.

(9) Jonoush, Z. A.; Rezaee, A.; Ghaffarinejad, A. Electrocatalytic nitrate reduction using Fe_0/Fe_3O_4 nanoparticles immobilized on nickel foam: Selectivity and energy consumption studies. *J. Cleaner Prod.* **2020,** *242*, 118569.

(10) Zhu, J. Y.; Xue, Q.; Xue, Y. Y.; Ding, Y.; Li, F. M.; Jin, P.; Chen, P.; Chen, Y. Iridium Nanotubes as Bifunctional Electrocatalysts for Oxygen Evolution and Nitrate Reduction Reactions. *ACS Appl. Mater. Interfaces* **2020,** *12* (12), 14064-14070.

(11) Duan, W.; Li, G.; Lei, Z.; Zhu, T.; Xue, Y.; Wei, C.; Feng, C. Highly active and durable carbon electrocatalyst for nitrate reduction reaction. *Water Res.* **2019,** *161*, 126-135.

(12) Gao, J.; Jiang, B.; Ni, C.; Qi, Y.; Zhang, Y.; Oturan, N.; Oturan, M. A. Non-precious Co_3O_4-TiO_2/Ti cathode based electrocatalytic nitrate reduction: Preparation, performance and mechanism. *Appl. Catal., B* **2019,** *254*, 391-402.